Biomechanical impact of the sclera on corneal deformation response to an air-puff: a finite-element study

B. Audrey Nguyen, Matthew A. Reilly, PhD, Cynthia J. Roberts, PhD

Purpose: To explore the impact of varying scleral properties on the corneal biomechanical behavior under loading by an air-puff using finite-element simulations.

Methods: Human donor eyes were mounted in a rigid fixture. One eye from each pair had its sclera stiffened with 1% or 4% glutaraldehyde, with the contralateral eye serving as control. A CorVis ST non-contact tonometer loaded the eye at several levels of intraocular pressure (IOP) and quantified the resulting deformation behavior. An axisymmetric, steady-state, and hyperelastic model was created using average dimensions for the adult human eye. The unloaded state of the eye was first estimated and assumed to represent a stress-free state. IOP was then applied to induce the residually stressed state. Finally, the eye was loaded by simulating the air-puff generated by the CorVis ST. IOP and scleral properties were varied between simulations.

Results: For each value of IOP tested, it was shown that increasing the ratio of scleral-to-corneal stiffness resulted in decreasing maximum apical displacement of the cornea. The model demonstrated that the stiffer the sclera, the higher the apparent stiffness of the whole eye. The model also showed that increasing the IOP while keeping material properties constant resulted in decreasing maximum apical displacement. The trends shown in the finite-element analysis were also observed in the experimental results from human donor eyes.

Conclusions: The finite-element model demonstrates that scleral material properties have an important impact on the biomechanical deformation response of the cornea in air-puff induced deformation. The observed biomechanical response of the cornea is a result of both corneal and scleral material properties, in addition to IOP.

Introduction

The study of ocular biomechanics has become and important part of vision research, and biomechanical markers are being explored to improve screening, diagnosis, and management of diseases such as keratoconus and glaucoma [1-11]. Increased understanding of corneal biomechanics is important for predicting outcomes of refractive surgery, and biomechanical properties of the sclera have been linked to glaucoma [2,4,6,8,12-13]. Much work has been done in the cornea, but fewer studies have looked at scleral biomechanics [3]. To our knowledge, a method for clinical evaluation of scleral properties has yet to be developed.

Several commercial devices have been developed which assess the biomechanical deformation response of the cornea, and provide insight into corneal biomechanical behavior *in vivo*. The Ocular Response Analyzer (ORA, Reichert Technologies) and the dynamic Scheimpflug analyzer CorVis ST (Oculus Optikgerate) are non-contact tonometers that both utilize an air-puff as the load on the cornea [14]. While the ORA can output a biomechanical parameter known as corneal hysteresis, defined as the difference between the first and second applanation pressures, its air puff will be different based on the timing of applanation in each eye [22]. In contrast, the CorVis ST outputs many dynamic corneal response (DCR) parameters based on image analysis, and its air-puff has been shown to be consistent and repeatable [23]. For this study, the CorVis ST was chosen for its consistent and reproduceable air-puff. Even with the recent advancements in the clinical assessment of corneal mechanics, there are no such devices that can characterize the *in vivo* biomechanical behavior of the sclera.

It has been shown that the biomechanical response of the cornea under air-puff deformation by the CorVis ST is significantly affected by the properties of the sclera [9]. Metzler et al showed that the human cornea behaves more stiffly in the case of a corneal button mounted on a rigid artificial anterior chamber (simulating stiffer scleral material properties) as opposed to an intact whole globe.

Biomechanical properties of ocular tissues are often determined by destructive *ex vivo* methods, which are greatly impacted by experimental conditions, including hydration state, strain rate, or the type of loading [2,4,16,17,24]. Finite element (FE) models and simulations have been explored as a way to evaluate *in vivo* properties of ocular tissues [3,4,15,18]. We present in this study a finite-element model and *ex vivo* experiment to explore the impact of varying scleral properties on the corneal biomechanical behavior under loading by an air-puff.

Methods

Ex vivo studies: Human donor eyes (n = 12 pairs) were obtained for this study from the Central Ohio Lions Eye Bank. Exclusion criteria included any previous ocular surgeries aside from cataracts surgery, and damage to the corneal epithelium. All experiments were conducted within 48 hours postmortem. The eyes were first injected and submerged in dextran solution (12.5% – 15% in PBS) to deswell the cornea. Central corneal thickness (CCT) was measured periodically by ultrasound pachymeter (DGH Pachette 2) until the CCT was approximately 550 microns. The whole globes were mounted using shallow sutures to a custom silicone-and-aluminum fixture and placed in front of the CorVis ST. A 20-gauge needle connected a saline column was inserted into the anterior chamber of the eye, and the height of the column was manipulated to simulate multiple levels of IOP (10, 20, 30, and 40 mmHg) during testing.

One eye from each matched pair was randomly selected for scleral stiffening using a glutaraldehyde crosslinking treatment. The treatment eye was submerged to the level of the limbus in a solution of 4% glutaraldehyde in PBS for 30 minutes. The fellow eye underwent a sham treatment with PBS alone. PBS was also dropped regularly onto the corneal surface to maintain adequate hydration. Dynamic corneal response (DCR) parameters were measured before and after scleral stiffening using the CorVis ST at all pressure steps, and at least three measurements of quality score “OK” was recorded for each pressure step.

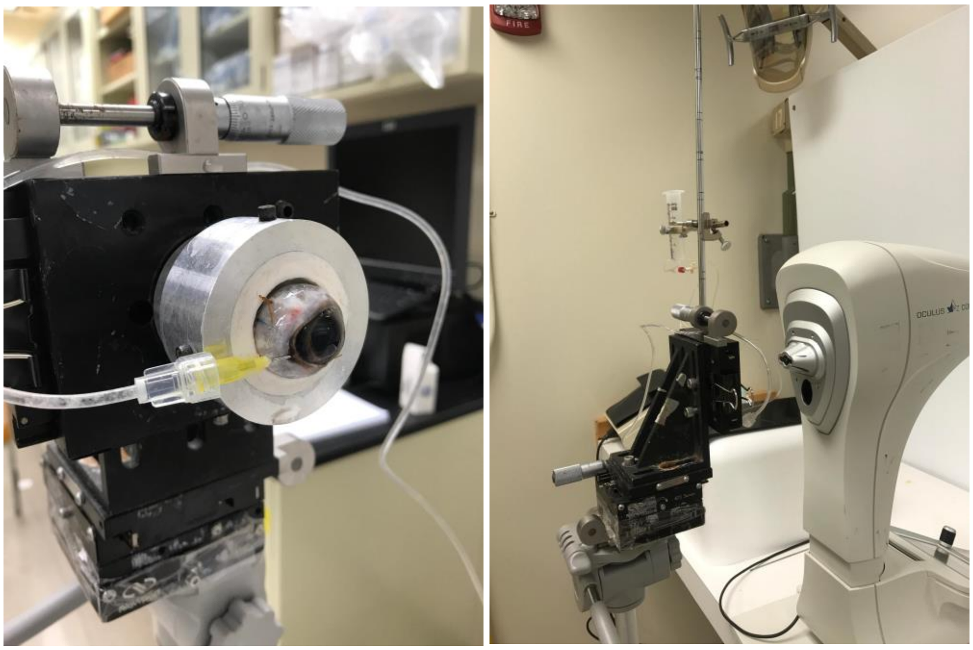

Figure 1: Whole globe mounted in custom holder (left) and *ex vivo* setup with CorVis ST (right)

Nasotemporal strips of corneal and scleral tissue were cut using mounted blades and measured by digital calipers for uniaxial tensile strip testing in a Rheometrics Systems Analyzer (RSA III). Each strip was preconditioned by alternating between loads of 0-gram-force (gf) to 5±1-gf. The strip was pre-loaded to 2.0-gf for 1 minute before a dynamic mechanical analysis (DMA) utilizing a sinusoidal wave with strain amplitude of 0.15% was performed. A second preload of 0.5-gf was applied for 5 minutes before tensile ramp testing was conducted. The ramp test was strain-controlled at a strain rate of 0.1% per second up to 6% strain. The stress-strain data were fit to a Neo-Hookean model to estimate the stiffness ratios of treated sclera to untreated cornea, and untreated sclera to untreated cornea.

Paired t-tests compared the change in DCRs following treatment (delta), and MANCOVA analyses were performed for selected DCRs as dependent variables, with IOP and estimated scleral stiffness as independent covariates.

Finite-element model: A 2D, axisymmetric, and steady-state model of the whole eye was constructed from average dimensions of the adult human eye in COMSOL. The "eye" comprised of the cornea, sclera, and vitreous humor, and the ocular tissues were modeled as hyperelastic and nearly incompressible, with material properties based on literature values [10-12].

Table 1: Summary of material properties for FE simulations

	Cornea	Sclera	Vitreous	Air
Young's Modulus (MPa)	1.5[5]	2.25, 3.0, 4.5, 6.0 [5]		-
Poisson Ratio	0.49	0.49	0.49	-
Bulk Modulus (MPa)	50.68	76.01	0.375[7]	-
Shear Modulus (Pa)	-	-	7.5	-
Density (kg/m3)	1050[6]	1100[6]	1000[7]	1.1855
Viscosity (Pa*s)			7.5E-4[7]	18.6E-6

Boundary conditions were chosen to replicate the *ex vivo* scleral experiments; the FE eye was fixed at the posterior to represent the whole globe being mounted in the rigid fixture, and the corneal apex was set at 11 mm from the CorVis ST nozzle. To explore the impact of scleral stiffening on corneal deformation, the material properties of the cornea and vitreous were held constant where those of the sclera were chosen to be either 1.5, 2, 3, or 4 times stiffer than the

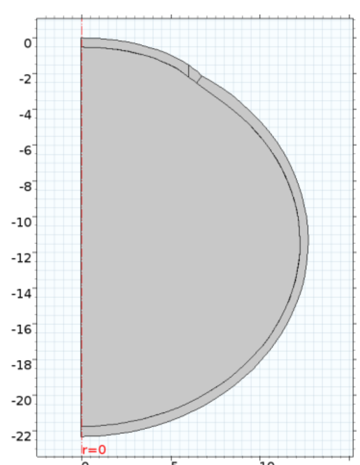

Figure 2: Finite-element model geometry of whole human eye

cornea. The IOP was also varied from 10 to 40 mmHg, in the same pressure steps as the *ex vivo* experiments.

Several steps were involved in the finite-element simulations. Firstly, the unloaded state of the must be estimated. The eye is naturally under tension while loaded by intraocular pressure, therefore the unloaded state was first estimated by applying a negative intraocular pressure to the interior corneoscleral boundary, with the resulting geometry assumed to represent a stress-free state. A positive IOP of the same magnitude was then applied to reinflate the eye, and to induce the residually stressed state. Finally, an air region was created surrounding the eye, and the eye was loaded by simulating the air-puff generated by the CorVis ST. The air-puff velocity and pressure profiles of the CorVis ST have been well characterized by hot-wire anemometry [23], and the simulated air-puff in the FE model was within 2% error of recorded measurements. The maximum apical displacement of the cornea was recorded for each simulation.

Figure 3: Recreated CorVis ST air-puff velocity and pressure profiles in COMSOL

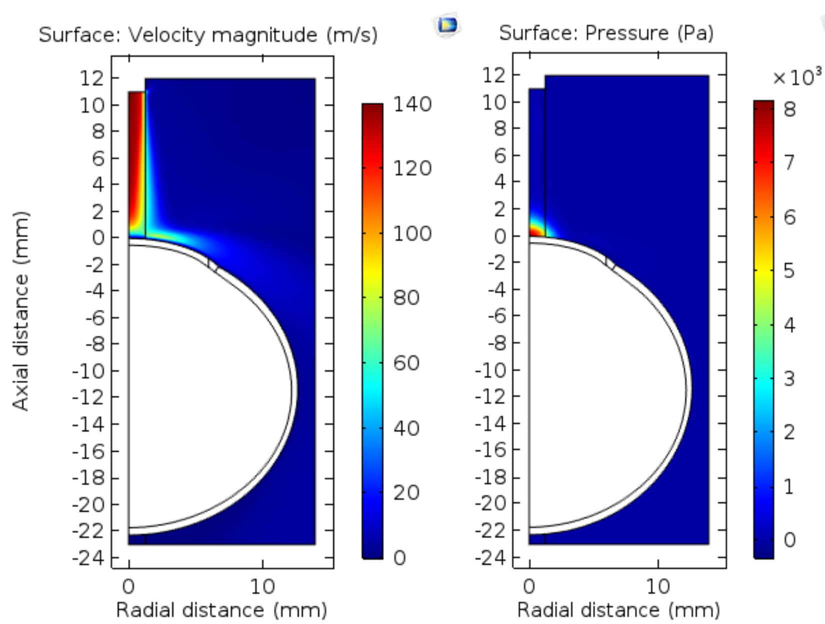

Results and Discussion

Mean treated and untreated sclera-to-cornea stiffness ratios were 6.7 and 2.6, respectively. Paired t-tests showed statistically significant ($p < 0.05$) decreases in the following DCRs at highest concavity (HC) and low IOP (10 mmHg) after scleral stiffening: maximum

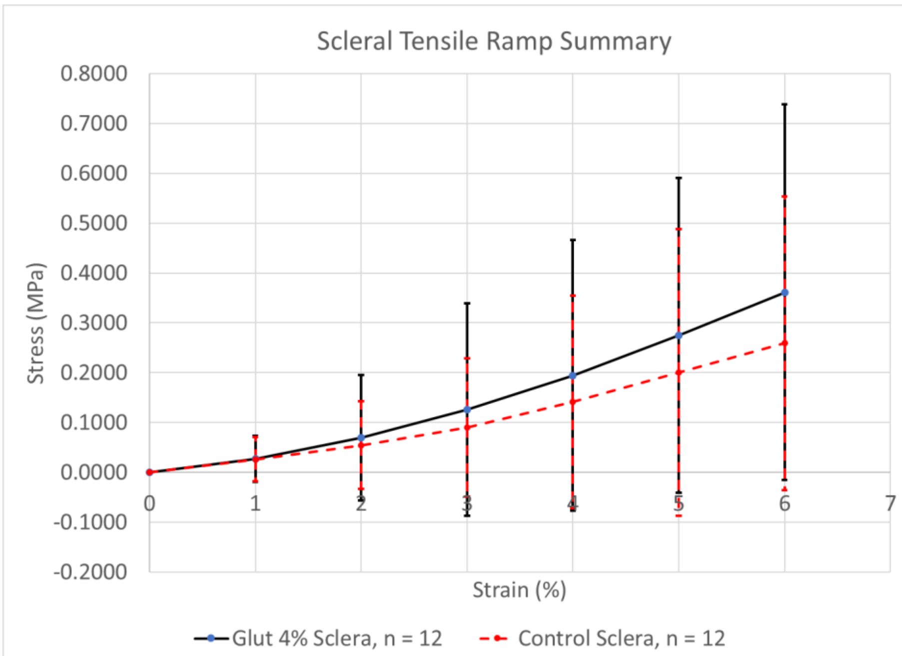

Figure 4: Summary of tensile ramp data from *ex vivo* experiments

deformation amplitude (DAmax), peak distance, and DA Ratio Max 2mm and 1mm. MANCOVA results showed significant relationships with both IOP and stiffness for all parameters listed and significant interaction between IOP and stiffness for DAmax. Decreasing values in highest concavity DCRs at IOP of 10 mmHg were predicted in the FE model.

Table 2: Summary of selected DCRs at highest concavity and 10 mmHg

Summary of selected DCRs at 10 mmHg				
	Def. Amp. Max [mm]	***Peak Dist. [mm]***	***DA Ratio Max (2mm)***	***DA Ratio Max (1mm)***
Avg value - Pre-treatment	1.476	5.868	4.575	1.583
Avg value - Post-treatment	1.224	5.493	4.367	1.565
Avg change - delta	-0.343	-0.495	-0.143	-0.017

The resultant geometries of the stress-free states were strongly impacted by both IOP and scleral-to-corneal stiffness, with the largest change in geometry occurring when IOP and scleral-to-corneal stiffness were maximized. When these resultant geometries were reinflated to induce the residually stressed states, the residual stresses followed a similar pattern to the stress-free geometries, in that higher IOP and scleral stiffnesses resulted in higher residual stresses.

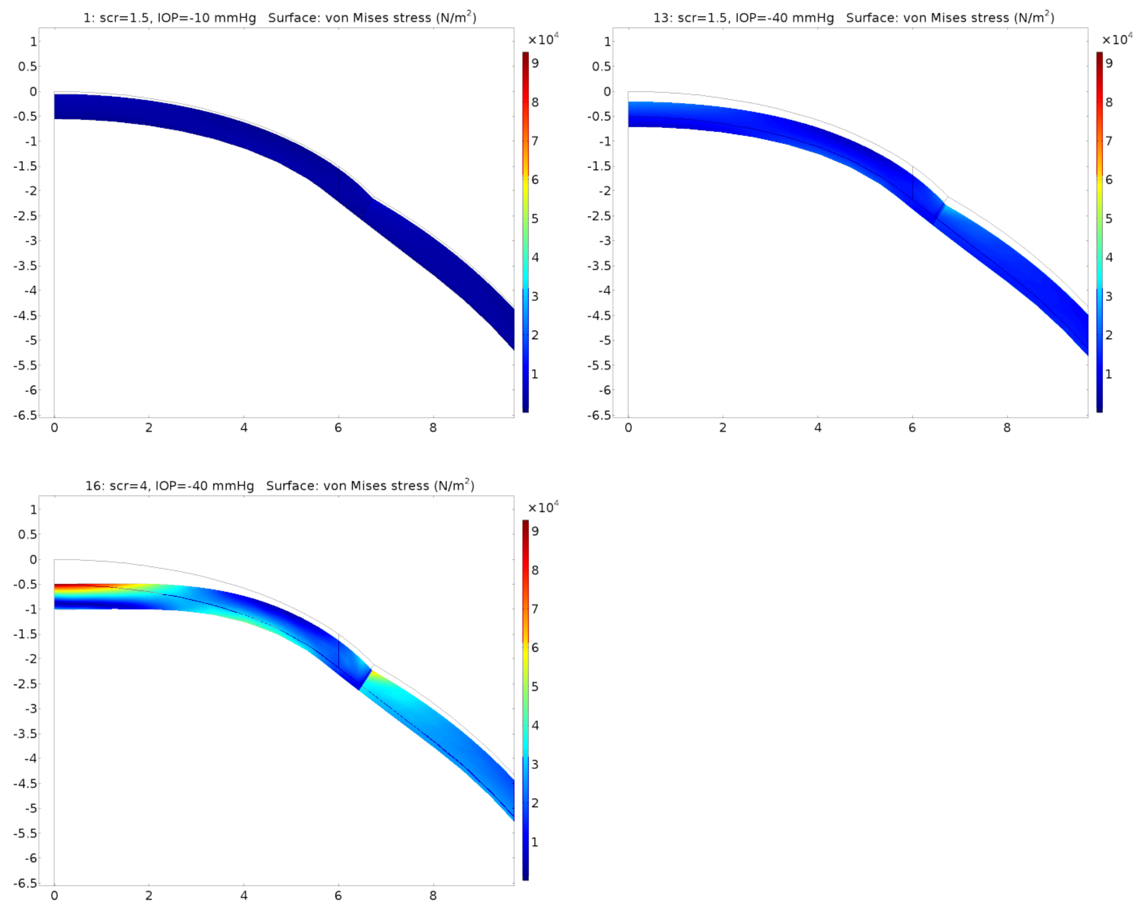

Figure 5: Resultant stress-free geometries with varying IOP and SCR

In the coupled deformation study, when the air-puff loading was simulated on the eye, higher stresses were observed at the posterior boundary of the cornea, as well as at the limbus (interface between cornea and sclera), and at the posterior sclera.

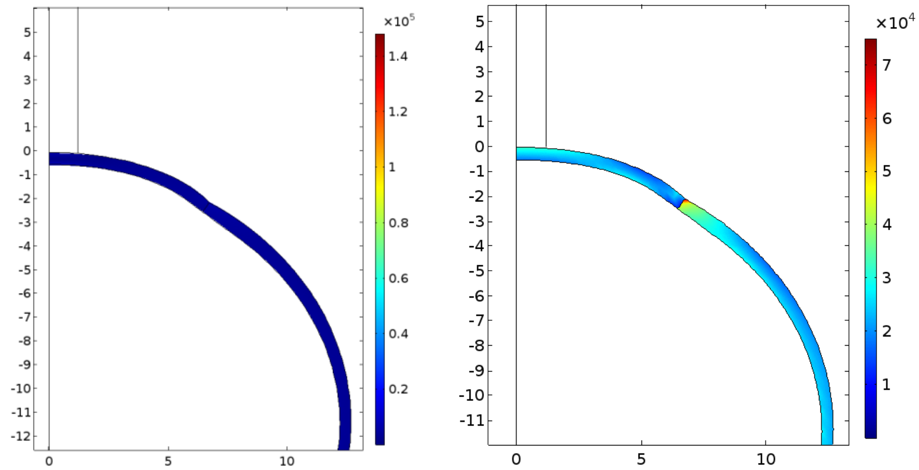

Figure 6: Resultant residually-stressed states; SCR 1.5 and IOP 10 mmHg (left), SCR 4.0 and IOP 40 mmHg (right)

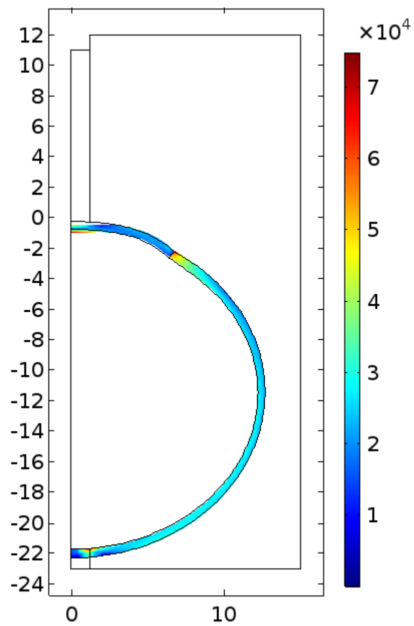

Figure 7: Stress distribution after coupled-deformation study

The maximum apical displacement of the cornea was recorded after each finite-element simulation. A contour plot of the results was generated in MATLAB. It was found that an increased scleral/corneal ratio resulted in decreased maximum apical displacement. Additionally, an increased IOP while maintaining constant material properties resulted in decreased maximum apical displacements. The trends observed in *ex vivo* experiments were predicted by the model.

Conclusions

We present a preliminary study that examines the impact of scleral stiffening on corneal biomechanical response to an air-puff. The experimental results demonstrate that stiffened sclera limits corneal deformation at lower IOP, and the simulation results of the FE model also predict these findings. Namely, the stiffer the sclera, the greater will be the limitation on corneal deformation by air-puff loading. This has important clinical implications and suggests that the observed corneal biomechanical response in air-puff induced deformation has contribution from both corneal and scleral material properties.

References:

1. Coudrillier B, Tian J, Alexander S, Myers KM, Quigley HA, Nguyen TD. Biomechanics of the human posterior sclera: age- and glaucoma-related changes measured using inflation testing. Invest Opthalmol Vis Sci 2012; 53(4):1714-1728.
2. Elsheikh A, Geraghty B, Alhasso D, Knappett J, Campanelli M, Rama P. Regional variation in the biomechanical properties of the human sclera. Exp Eye Res 2009; 90:624-633.
3. Girard MJA, Dupps WJ, Baskaran M, Scarcelli G, Yun SH, Quigley HA, Sigal IA, Strouthidis NG. Translating ocular biomechanics into clinical practice: current state and future prospects. Current Eye Research 2015; 40:1-18.
4. Liu J, Roberts CJ. Influence of corneal biomechanical properties on intraocular pressure measurement: quantitative analysis. JCRS 2005; 31:146-155.
5. Roberts CJ. Importance of accurately assessing biomechanics of the cornea. Curr Opin Ophthalmology 2016; 27:000-000.
6. Norman RE, Flanagan JG, Rausch SMK, Sigal IA, Tertinegg I, Eilaghi A, Portnoy S, Sled JG, Ethier CR. Dimensions of the human sclera: thickness measurement and regional changes with axial length. Exp Eye Research 2010; 90:277-284.
7. Pavlatos E, Perez BC, Morris HJ, Chen H, Palko JR, Pan X, Weber PA, Hart RT, Liu J. Three-dimensional strains in human posterior sclera using ultrasound speckle tracking. J Biomech Eng 2015; 138(2):021015-021015-9.
8. Elsheikh A, Whitford C, Hamarashid R, Kassem W, Joda A, Buchler P. Stress free configuration of the human eye. Med Eng Phy 2013; 35:211-216.
9. Roberts CJ. Concepts and misconceptions in corneal biomechanics. JCRS 2014; 40:862-869.
10. CT McKee, JA Last, P Russel, CJ Murphy. Indentation versus tensile measurements of Young’s modulus for soft biological tissues. Tissue Engineering Part B, 2011; 17(3): 156-64.
11. EYK Ng and EH Ooi, FEM simulation of te eye structure with bioheat analysis. Computer Methods and Programming in Biomedical Engineering, 2006; 82(3): 268-76.
12. JJ Heys, VH Barocas, MJ Taravella, Modeling Passive Mechanical Interaction between aqueous humor and iris. Journal of Biomedical Engineering, 2001; 123: 540-47.